A Kinetic Model To Simulate Protein Crystal Growth in an Evaporation-Based Crystallization Platform

Sameer Talreja,[†] Paul J. A. Kenis,*[,†,‡] and Charles F. Zukoski*[,†,§]

Department of Chemical and Biomolecular Engineering, Center for Biophysics and Computational Biology, and Institute for Genomic Biology and Beckman Institute, University of Illinois at Urbana-Champaign, 600 South Matthews Avenue, Urbana, Illinois 61801

Received December 25, 2006. In Final Form: January 23, 2007

The quality, size, and number of protein crystals grown under conditions of continuous solvent extraction are dependent on the rate of solvent extraction and the initial protein and salt concentration. An increase in the rate of solvent extraction leads to a larger number of crystals. The number of crystals decreases, however, when the experiment is started with an initial protein concentration that is closer to the solubility boundary. Here we develop a kinetic model capable of predicting changes in the number and size of protein crystals as a function of time under continuous evaporation. Moreover, this model successfully predicts the initial condition of drops that will result in gel formation. We test this model with experimental crystal growth data of hen egg white lysozyme for which crystal nucleation and growth rate parameters are known from other studies. The predicted and observed rates of crystal growth are in excellent agreement, which suggests that kinetic constants for nucleation and crystal growth for different proteins can be extracted by applying a kinetic model in combination with observations from a few evaporation-based crystallization experiments.

1. Introduction

Proteins are notoriously difficult to crystallize, so much so that current methods rely on high-throughput screening technologies in which hundreds to thousands of solution conditions are screened in the hope that the conditions suitable to produce X-ray diffraction quality crystals will be identified. This process is slow and represents a major bottleneck in linking protein structure to function.[1] Even when suitable solution conditions for crystal formation are found, the quality (size, polymorph, and degree of internal order) is sensitive to the method by which supersaturation is achieved.[2,3] Recently we demonstrated that manipulating the rate of solvent evaporation from small drops enables systematic study of the effect of the rate of supersaturation on the number and size of protein crystals formed.[4] Kinetic models that describe the rates of supersaturation, crystal nucleation, and growth are needed to gain deeper insight into the fundamental rate processes occurring in the regulated-evaporation crystallization process.

The "hanging drop technique" is frequently used to grow protein crystals.[1] Small drops containing protein and precipitant are allowed to equilibrate by vapor diffusion with a solution of a lower initial chemical potential of the solvent. Extending this concept, we have developed a method that ensures the formation of a solid phase in each drop, and, as a result, each experiment yields information on crystal solubility, as well as on crystal nucleation and growth rates.[4] This method employs evaporation of the solvent from a drop at a predetermined, constant rate, set by the length and area of a microfabricated channel that connects the crystallization compartment with the ambient atmosphere (Figure 1a). This method yields different solid phases, including amorphous precipitates, gels, showers of small crystals, a few larger crystals, or combinations of those depending on the initial protein and precipitant concentrations and the rate of drying. Once conditions resulting in crystals have been identified, the crystal size can be monitored as a function of time during the drying process. In this paper we use empirical expressions for

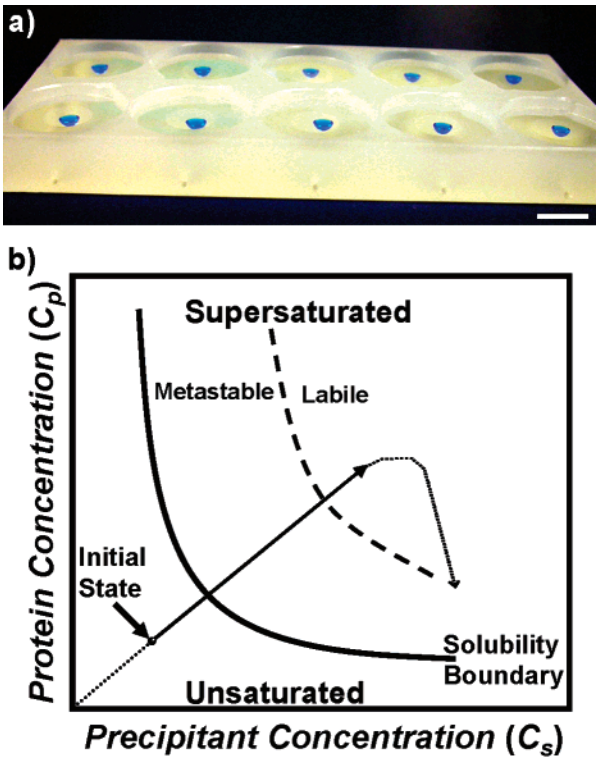

Figure 1. (a) Optical micrograph of a polypropylene crystallization platform with 2 × 5 crystallization compartments as used in this study. Scale bar: 1 cm. (b) Protein versus salt concentration profile in the evaporation experiment as the solvent evaporates and crystals form.

* Corresponding author. E-mail: czukoski@uiuc.edu (C.F.Z.); kenis@uiuc.edu (P.J.A.K.).
[†] Department of Chemical and Biomolecular Engineering.
[‡] Institute for Genomic Biology and Beckman Institute.
[§] Center for Biophysics and Computational Biology.

(1) McPherson, A. *Crystallization of Biological Macromolecules*, 3rd ed.; Cold Spring Harbor Laboratory Press: Cold Spring Harbor, New York, 1999.
(2) Chayen, N. E. *J. Appl. Crystallogr.* **1997**, *30*, 198−202.
(3) Chayen, N. E. *Structure*. **1997**, *5*, 1269−1274.
(4) Talreja, S.; Kim, D. Y.; Mirarefi, A. Y.; Zukoski, C. F.; Kenis, P. J. A. *J. Appl. Crystallogr*. **2005**, *38*, 988−995.

10.1021/la063734j CCC: $37.00
Published on Web 03/17/2007

nucleation and growth rates as available in the literature[5] and apply them in a new model to simulate the crystal nucleation and growth process of the commonly studied protein lysozyme in the evaporation-based crystallization platform and compare results of this model with experimental crystal growth data.

2. Model Development

The model developed in this work is a statement of the conservation of mass of solute present in the drop as it progresses from the soluble to crystalline form. The crystals grow at a rate defined as $G(t)$, and the number of crystals nucleated per unit volume per unit time is defined as $B(t)$. We choose the following common equations to relate the nucleation and growth rates to the protein concentration in the droplet:[6]

$$B(t) = k_n\left(\frac{C_p(t) - C_{sat.}(t)}{C_{sat.}(t)}\right)^a = k_n(S(t) - 1)^a \quad (1a)$$

$$G(t) = \frac{dl_c}{dt} = k_g\left(\frac{C_p(t) - C_{sat.}(t)}{C_{sat.}(t)}\right)^b = k_g(S(t) - 1)^b \quad (1b)$$

where l_c is the characteristic length of a crystal, $C_p(t)$ and $C_{sat.}(t)$ are the protein concentration and protein solubility, respectively, as appropriate for solution conditions at time t, and $S(t)$ is the supersaturation as defined by $S(t) = C_p(t)/C_{sat.}(t)$. The parameters k_n and k_g are the crystal nucleation and growth rate constants, respectively, and a and b are constants. In eq 1a and eq 1b we denote explicit time dependencies to emphasize that in the evaporation-based crystallization procedure used here the supersaturation and thus the rates of nucleation and growth continuously change as the solvent evaporates with time.

Assuming ideal volumes of mixing, the total volume of the drop V equals $V_{solvent}(1 + V_p/V_{solvent} + V_s/V_{solvent})$, where V_p and V_s represent the volume occupied by protein and salt, respectively, and $V_{solvent}$ is the volume occupied by solvent at any time. We assume that the rate of solvent evaporation is constant, which enables us to write a linear expression for the volume of the drop at any time t as $V = V_{solvent}(1-\alpha t)$, which for dilute drop conditions can be written as $V_0(1\text{-}\alpha t)$, where V_0 is the initial volume of the drop and α is a time constant such that at $\alpha t = 1$ the drop is completely dry. Conditions where the rate of solvent evaporation is constant are achieved only for dilute solutions where the activity of water is not greatly influenced by the presence of the solutes (protein and salt). In other words, the rate of solvent evaporation from the drop will be constant to the point where the concentration of solute in the drop does not significantly reduce the equilibrium vapor pressure above the drop from that of the vapor pressure above the initial drop. As a result our analysis is only applicable when $(V_p + V_s)/V_{solvent}$ is small.[7,8] To satisfy this condition, we apply the model only up to dimensionless time $t^* = \alpha t = 0.85$, after which the amount of salt and protein becomes comparable to the amount of water present in the drop.[9] The mass balance for the protein in the drop can be written as

$$\frac{d(C_p(t) + W(t))}{dt} = \frac{C_{p0}\alpha}{(1 - \alpha t)^2} \quad (2)$$

where $C_p(t)$ is the soluble protein concentration, $W(t)$ is the mass concentration of protein in crystalline form and C_{p0} is the initial protein concentration. Using $S(t) = C_p(t)/C_{sat.}(t)$ eq 2 can be rewritten as

$$\frac{dS}{dt} = \frac{C_{p0}\alpha}{C_{sat.}(1 - \alpha t)^2} - \frac{1}{C_{sat.}}\frac{dW}{dt} - \frac{S}{C_{sat.}}\frac{dC_{sat.}}{dt} \quad (3)$$

In this work we assume that the solubility of the protein $C_{sat.}(t)$ is a function of the concentration of a nonvolatile solute, in this case a salt. As the water leaves the drop, the salt concentration, $C_s(t)$, increases which results in changes in $C_{sat.}(t)$. When using a simple electrolyte as the precipitant, the protein solubility can be expressed as

$$C_{sat.}(t) = \varphi \exp(-\beta C_s(t)) \quad (4a)$$

where φ and β are constants.[1,10] Since the mass of salt in the drop is constant but the volume of the drop changes as $V_0(1-\alpha t)$, $C_s(t)$ can be written as

$$C_s(t) = \frac{C_{s0}}{(1 - \alpha t)} \quad (4b)$$

Substituting eq 4b in eq 4a and differentiating

$$\frac{dC_{sat.}}{dt} = -\frac{\beta C_{sat.}\alpha C_{s0}}{(1 - \alpha t)^2} \quad (4c)$$

Substituting eq 4c in eq 3 provides a different expression for the rate of supersaturation:

$$\frac{dS}{dt} = \frac{C_{p0}\alpha}{C_{sat.}(1 - \alpha t)^2} - \frac{1}{C_{sat.}}\frac{dW}{dt} + \frac{\beta S\alpha C_{s0}}{(1 - \alpha t)^2} \quad (5)$$

For the crystals in solution we define N as the number of crystals, l as the total characteristic length of the crystals, A as the total area of crystals, and W as the total mass of crystals. Assuming nuclei to be of zero size,[5] the nucleation and growth rate are defined as

$$\frac{dN}{dt} = \begin{cases} B(t), & l_c = 0 \\ 0, & l_c > 0 \end{cases} \quad (6a)$$

$$\frac{dl}{dt} = NG(t) \quad (6b)$$

Assuming that the crystals in our study will be geometrically similar, the mass of each crystal (W_c) can be related to its characteristic length (l_c):

$$W = NW_c = \rho k_v l_c^3 N \quad (6c)$$

where ρ_c is the crystal density and k_v is a volumetric shape factor. The shape factor is independent of size for geometrically similar particles. Differentiating eq 6c with respect to time and using the definition of $G(t)$ (eq 1b) and $l = Nl_c$, provides an expression for the change of mass of protein crystals with time:

$$\frac{dW}{dt} = 3\rho_c k_v \frac{l^2}{N} G(t) \quad (6d)$$

(5) Randolph, A. D.; Larson, M. A. *Theory of Particulate Processes*; Academic Press: New York, 1971; pp 53−63.
(6) Saikumar, M. V.; Glatz, C. E.; Larson, M. A. *J. Cryst. Growth* **1998**, *187*, 277−288.
(7) Kreidenweis, S. M.; Koehler, K.; DeMott, P. J.; Prenni, A. J.; Carrico, C.; Ervens, B. *Atmos. Chem. Phys.* **2005**, *5*, 1357−1370.
(8) Blandamer, M. J.; Engberts, J.; Gleeson, P. T.; Reis, J. C. R. *Chem. Soc. Rev.* **2005**, *34*, 440−458.
(9) Fowlis, W. W.; Delucas, L. J.; Twigg, P. J.; Howard, S. B.; Meehan, E. J.; Baird, J. K. *J. Cryst. Growth* **1988**, *90*, 117−129.
(10) Rosenbaum, D.; Zamora, P. C.; Zukoski, C. F. *Phys. Rev. Letter*. **1996**, *76*, 150−153.

Table 1. Kinetic Parameters (k_n, k_g, a, b) for Lysozyme Crystallization and the Constants (φ, β, k_v, ρ) Used in the Model As Taken from the Literature[1,6,10]

k_n	7.71×10^{-2}/h	φ	894.56 mg/mL
k_g	1.37×10^{-4} cm/h	β	6.2528 mL/mg
a	3	k_v	1
b	2	ρ	1.45 g/mL

Equation 5 and eqs 6a−d provide a closed set of differential equations that can be solved to predict the behavior of the drying drops. Here we apply the initial conditions of $l = A = N = 0$ at $t \leq t_{sat.}$, where $t_{sat.}$ is the time when $C_p = C_{sat.}$.

The model requires six parameters for quantitative predictions: k_n, k_g, a, b, φ, and β. For lysozyme, we use values for the parameters k_n, k_g, a, b and the constants k_v, ρ_c from work by Saikumar et al.[6] and we calculate φ and β using experimental solubility data from Rosenbaum et al.,[10] as summarized in Table 1.

3. Experimental Section

3.1. Crystallization Experiments. For the crystallization experiments reported in this work, we used an evaporation-based crystallization platform with 10 crystallization compartments each connected to a channel with a cross-sectional area (A_c) of 0.3 mm^2 and a length (L) of 5 mm. We have reported the fabrication and characterization of this platform previously.[4] The evaporation rate, J, was determined empirically to be 4.2×10^{-2} μL/h for the channels used in this study when drying took place with an external relative humidity of 30%. The external relative humidity was held constant for all experiments reported here. The drying times for a drop of pure water and a drop containing different solutes differed less than 2% from each other, indicating that the decrease in water activity at the end of the drying process has negligible effect on the overall drying time.

For the experiments described here, 40 mg/mL lysozyme protein (Seikagaku America, Falmouth, MA) was suspended in 50 mM acetate buffer, obtained from acetic acid and sodium acetate (Fischer Scientific, Pittsburgh, PA), at pH 4.6 with the initial salt concentration C_{s0} ranging from 0.4 to 1.5 M. NaCl (Sigma, St. Louis, MO) was used as the precipitant. Prior to mixing and setting up the experiment, both the NaCl and lysozyme solution were filtered (0.02 μm pores, Anotop 25 Whatman, Maidstone, England). Lysozyme concentrations were determined by absorbance measurements at 280 nm using an extinction coefficient for lysozyme of 2.64 mL/(mg.cm).[11,12] Dilutions of this stock solution with acetate buffer yielded solutions of the same C_p/C_s ratio but different C_{p0}. Droplets were formed by placing 5 μL of these stock solutions on silanized glass slides (Hampton Research, Laguna Niguel, CA) with a 0.5−10 μL micropipette (Thermo Labsystems Finpipette, Waltham, MA) and these slides were inverted on the crystallization compartments. The droplets were then followed over time with a Leica MZ-12 stereozoom microscope equipped with a Sony DXC-390 CCD camera. The growth rates of individual crystals were determined using the image analysis software *ImageJ* (The National Institute of Health, Bethesda, MD), which enables determination of particle size in an image. We define the characteristic length of the crystal as the average of the length and the width of the visible face of the crystal. The total number of crystals formed was counted from the images taken with the stereozoom microscope.

3.2. In Situ Monitoring Equipment. High-throughput crystallization experiments were realized using an automatic imaging system (AIS) that comprises four major components: an optical microscope (Leica Z16 APO) equipped with an autozoom lens that magnifies the samples; a CMOS digital camera (Leica DFC280) that captures images; a motorized stage (Semprex KL66) that moves in X and Y directions to facilitate automatic experimental observation of many experiments in rapid sequence; and a personal computer that controls all the peripherals through relevant software packages. This programmable AIS is able to monitor hundreds of experiments in autonomous fashion by sequentially moving from one compartment to the next, capturing and storing multiple images at each compartment.

3.3. Model Simulations. The model as explained in section 2 was compiled in computer code using the software package MATLAB (MathWorks Inc., Natick, MA).

4. Results and Discussion

Figure 1a shows a 2 × 5 multicompartment evaporation-based crystallization platform that we used in this study. Each crystallization experiment starts at a certain initial protein and precipitant concentration.[4] We use salt as a precipitant and denote its concentration as C_s in concentration units of molar (M). We express the protein concentration in units of milligrams per milliliter. Figure 1b shows the state of the drop during the evaporation-based crystallization experiment. Initial drying takes place at a constant ratio of C_p/C_s, and at some point the solubility line ($S = 1$) is crossed. Further drying yields a supersaturated solution, thus producing a driving force for protein crystals to form. Once crystal nucleation and growth sets in, the supersaturation in the drop depends on two opposing effects: (i) an increase in total protein and salt concentration in the drop due to solvent evaporation and (ii) a decrease in protein concentration in solution due to nucleation and growth of crystals. These two opposing effects cause the supersaturation to go through a maximum at some point in time.

Experiments were performed at different initial conditions of salt and protein concentrations. The dimensions of the crystals were measured as a function of time for those drops in which crystals did form. Figure 2 shows the variation of crystal size with different initial protein and salt concentration and C_p/C_s ratios for a fixed α. Note that in Figure 2a−d the time axis is expressed in the dimensionless form, $t^* = \alpha t$. The characteristic length of the crystal was taken as the average of the length and the width of the visible face of the crystal. In our experiments we varied the C_p/C_s ratio from 30 to 100 g/mol and C_{p0} from 10 to 30 mg/mL. Drying was carried out at a constant evaporation rate of 4.2×10^{-2} μL/h, which corresponds to $\alpha = 8.3 \times 10^{-3}$ h^{-1}.

Given the small volume of the droplet used in each experiment and the resulting small number of crystals, a set of experiments was performed with identical initial conditions to confirm reproducibility. We observe the same number (three) of crystals (Figure 3a) and a very narrow distribution of $l(t^*)$ in six experiments of drying 5 μL drops with $C_p/C_s = 100$ g/mol and $C_{p0} = 22$ mg/mL (Figure 3b).

Figure 2 also shows predicted values of crystal size as a function of time as obtained with the model (eq 5 and eq 6) described in section 2 above using values for k_n, k_g, a, and b from the literature.[6] Saikumar et al.[6] obtained these parameters by using the population balance model in combination with experimental observation of the number and size of crystals formed. These experiments were performed using 1 mL of protein/precipitant mixture in a polyethylene transfer pipet, heat-sealed at both ends. The experimental data of crystal growth obtained in our study with the evaporation-based crystallization platform and our model predictions are in excellent agreement with each other. This agreement indicates that despite the vastly different crystallizer volumes and different methods of creating supersaturation, the kinetic parameters provide a robust description of crystal nucleation and growth.

The state of the protein in the droplet is determined by a competition between the rate of change in average concentration,

(11) Boyer, P. M.; Hsu, J. T. *Chem. Eng. Sci*. **1992**, *47*, 241−251.
(12) Boyer, P. M.; Hsu, J. T. *Biotechnol. Tech.* **1990**, *4*, 61−66.

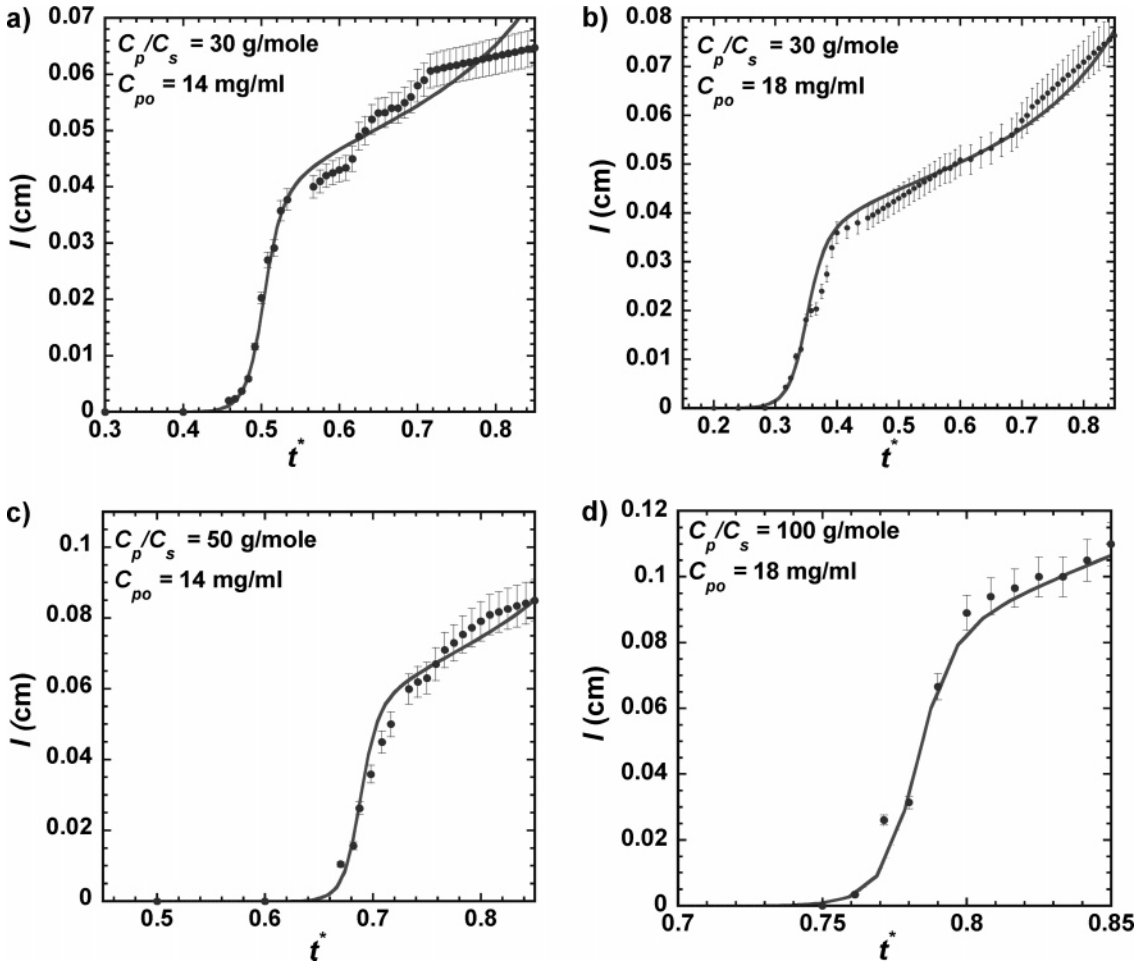

Figure 2. Comparison of experimentally measured (dots) and theoretically predicted (solid curve) crystal lengths of lysozyme crystals obtained from drops with different initial conditions. (a) C_p/C_s = 30 g/mol, C_{p0} = 14 mg/mL; (b) 30 g/mol, 18 mg/mL; (c) 50 g/mol, 14 mg/mL; and (d) 100 g/mol, 18 mg/mL. The parameters used in these model calculations are listed in Table 1. Drying was carried out at a constant evaporation rate of 0.042 μL/h, which corresponds to $\alpha = 0.0083$ h^{-1}.

nucleation, growth, and gel formation. The rate of solvent evaporation and the initial protein and salt concentrations are the variables that can be changed to achieve the desired crystal properties. In prior work we have shown that experiments starting with different initial conditions but identical, fixed C_p/C_s (conditions a−c in Figure 4) will all traverse the same path and will all cross point f in Figure 4.[4] Figure 5 shows the result at point f for experiments that started as 5 μL drops with C_{p0} of 2, 14, and 32 mg/mL and C_{s0} of 0.02, 0.14, and 0.32 M, respectively, so C_p/C_s is 100 for all. Gels and films are formed when C_{p0} is small, but initial protein concentrations C_{p0} that are closer to the solubility boundary result in an increasing number of crystals. Qualitatively the differences in state of the solids at point f can be understood by recognizing that once the solubility boundary is crossed, the number and size of crystals depends on the magnitude of four rates: (i) the rate of nucleation at a given supersaturation, (ii) the rate of growth at a given supersaturation, (iii) the rate of localization (or gelation), and (iv) the rate of change of supersaturation. In the evaporation method modeled here, the rate of nucleation drops to negligible rates when the total crystal surface area reaches a point such that the rate of transfer of protein from solution to a crystal surface equals or exceeds the rate of increase in the protein concentration as a result of solvent evaporation. The number of crystals formed increases with an increase in the maximum supersaturation reached. This competition between evaporation and, nucleation and growth result in different states (film, gel, precipitate, and crystals, etc.), as shown in Figure 4. The same effects are observed in a set of experiments that all start at condition *a*, but each have different predetermined rates of evaporation. For lysozyme, more and small crystals are formed as the rate of change in protein concentration increases or a higher supersaturation is reached.

Figure 6 shows predictions of the number and the length of crystals as well as supersaturation profiles based on the kinetic model for initial conditions corresponding to the data in Figure 5. As before, the kinetic and thermodynamic parameters used in the simulations are taken from work by Saikumar et al.[6] as summarized in Table 1. As expected the common features as seen from Figure 6a−c are that *S* increases to a maximum before decreasing to a minimum after which *S* increases again. The initial increase in *S* results from a decrease in drop volume due to evaporation. The maximum in *S* corresponds to the time when the number of crystals and their growth has reached sufficiently high values such that the decrease in protein concentration due to crystal growth is comparable to the increase in protein concentration due to drying. The subsequent decrease in *S* is the result of the reduction in protein concentration due to crystal growth exceeding the increase in protein concentration due to drying. The final increase in *S* occurs because the drop volume is so small that small amounts of evaporation dramatically increase the protein concentration. Of interest here is the case where high supersaturation on the order of 10−40 is predicted (Figure 6a). Such large values of *S* are unusual for small molecules but

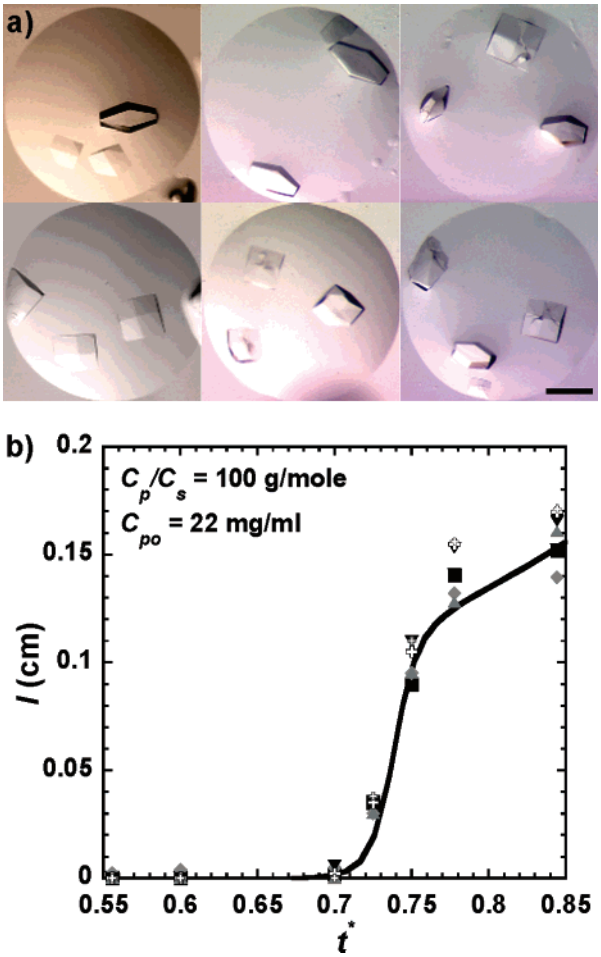

Figure 3. (a) Optical micrographs of droplets from six experiments with identical initial conditions (C_p/C_s =100 g/mol, C_{p0} = 22 mg/mL) with $\alpha = 0.0083\ h^{-1}$. Scale bar: 500 μm. (b) The crystal length l as a function of dimensionless time t^* for the six experiments shown in a. The solid line indicates the model prediction using the parameters listed in Table 1.

solutions of lysozyme with supersaturation of 8 have been reported to show no signs of nucleation or cluster formation for several months.[13,14]

As shown in Figure 6b, the number of crystals produced by the drying process are predicted to increase as C_{p0} decreases, while Figure 6c predicts that the total length l at $t^* = 0.85$ increases for experiments in which C_{p0} is closer to $C_{sat.}$ at a fixed C_p/C_s ratio. For each experiment, the maximum in S (Figure 6a) corresponds to an upturn in $l(t)$ (Figure 6b), indicating substantial growth of crystals at this time. Also, the model successfully predicts the number of crystals to within ±1 of the observed number. Similarly, in identical experiments we observe the same number of crystals with a variation of ±1. In Figure 6b, the number of crystals as predicted by the model is represented as a continuous function of time. To compare the model predictions with the experimental observation we use the model prediction values at $t^* = 0.85$. The model predicts three crystals for C_{p0} = 14 mg/mL and two crystals for the condition C_{p0} = 32 mg/mL (Figure 6b), and in our experiments we observe two and four crystals, respectively (Figure 5b,c).

The prediction of the number and the length of crystals in Figure 6b,c qualitatively captures the experimental observation,

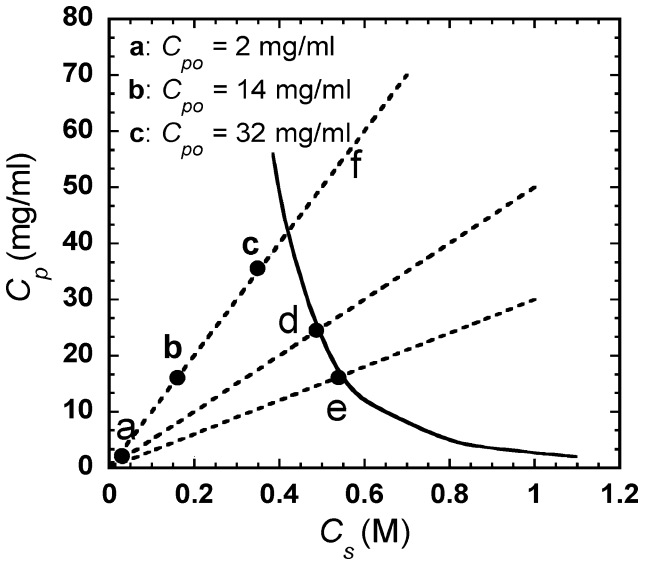

Figure 4. Paths to supersaturation as plotted in a lysozyme concentration (C_p) vs NaCl concentration (C_s) graph. The solid line ($S = 1$) represents the solubility boundary. The dotted lines represent paths of different C_p/C_s ratios (30, 50, and 100 g/mol) along which different experiments are performed. Points a−c indicate initial conditions of C_{p0} = 32, 14, and 2 mg/mL, of three different experiments. The experiments that originate in points a−c eventually will pass though point f.

as shown in Figure 5, except at the lowest C_{p0}, where, under a variety of salt concentrations, a film or gel is observed.[15] Gelation is associated with large strengths of attraction between protein molecules and the presence of high protein concentrations. It typically occurs under conditions where the protein solution is supersaturated with respect to crystal formation. Thus reversible gels formed by globular proteins are seen when concentrated protein solutions are rapidly quenched such that a non-ergodic phase forms more rapidly than crystals can nucleate.[14] Crystallization is associated with protein molecules assembling into an orientationally ordered state requiring many diffusion attempts before a critical nucleus is formed. On the other hand, localization is associated with an inability to diffuse out of a cage of nearest neighbors with no barrier to cluster formation. Thus, once the average strength of attraction reaches a critical, large value, gelation may be expected to occur more rapidly than crystal nucleation. In our system gels are formed if the time to reach the value of S that defines the gel boundary is less than what is required for at least one nucleus to form. We hypothesize that such conditions are reached for the case where $C_{p0} = 2$ mg/mL, as shown in Figure 6a for which the model predicts a maximum supersaturation of 40.

To demonstrate our hypothesis, we turn to the analysis where proteins are treated as hard-core particles experiencing short-range interactions.[16−19] The square-well interaction energy, $U(r)$, captures the essential features of protein solution thermodynamics:[17]

$$\frac{U(r)}{kT} = \begin{cases} \infty & r \le \sigma \\ -\epsilon/kT & \sigma < r \le \sigma(1+\Delta) \\ 0 & r > \sigma(1+\Delta) \end{cases} \qquad (7)$$

where r is the center-to-center separation of a pair of particles,

(13) Zukoski, C. F.; Kulkarni, A. M.; Dixit, N. M. *Colloids Surf., A* **2003**, *215*, 137−140.
(14) Kulkarni, A. M.; Dixit, N. M.; Zukoski, C. F. *Faraday Discuss.* **2003**, *123*, 37−50.
(15) Dixit, N. M.; Zukoski, C. F. *Phys. Rev. E* **2003**, *67*.
(16) Bonnete, F.; Vivares, D. *Acta Crystallogr., Sect. D: Biol. Crystallogr.* **2002**, *58*, 1571−1575.
(17) Rosenbaum, D. F.; Kulkarni, A.; Ramakrishnan, S.; Zukoski, C. F. *J. Chem. Phys.* **1999**, *111*, 9882−9890.

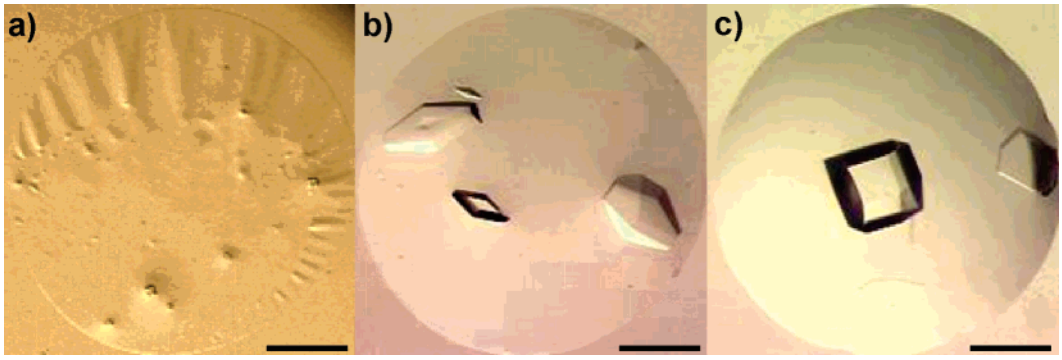

Figure 5. Optical micrographs of droplets at condition f in Figure 4 for drops starting from initial conditions of C_{p0} of 2, 14, and 32 mg/mL (points a−c in Figure 4) with $C_p/C_s = 100$ g/mol. Drying was carried out at a constant evaporation rate of 0.042 μL/h. At point f the drops have the same average protein concentration. The difference observed in the drops is due to the different rates at which the drops pass through state f. Scale bar: 500 μm.

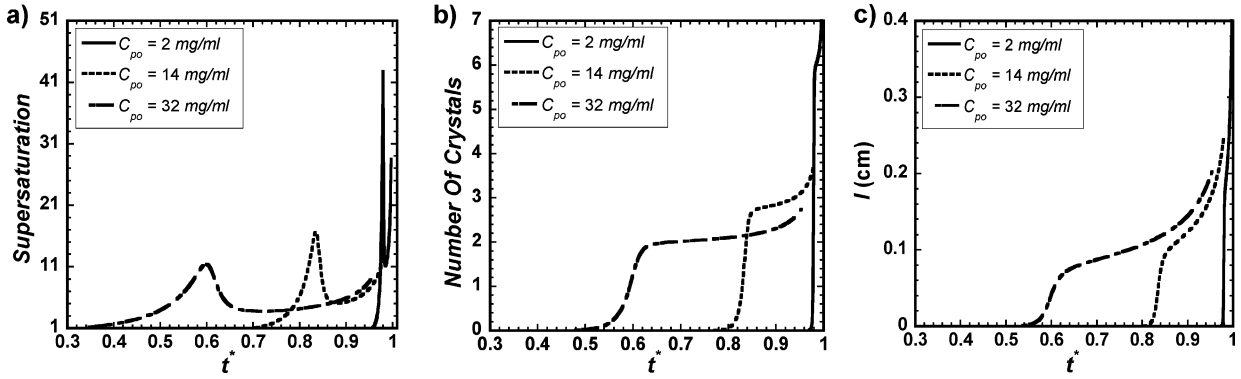

Figure 6. Prediction of (a) supersaturation S vs dimensionless time t^*: (b) number of crystals N vs dimensionless time t^*; (c) total length of crystals l vs dimensionless time t^* for initial conditions a−c shown in Figure 5. The drop is completely dry at $t^* = 1$.

ϵ is the strength of attraction between the particles of diameter σ, and Δ is the range of attraction. Here kT is the product of Boltzmann's constant and the absolute temperature.[14] Bergenholz and Fuchs[20−22] developed an analytical expression, eq 8a, for gelation of weakly attractive particles experiencing square-well attractions by applying idealized mode-coupling theory (MCT):[14]

$$\frac{12\Delta\varphi_{gel}}{\pi^2}\left[\exp\left(\frac{\epsilon}{kT}\right) - 1\right]^2 = 1.42 \qquad (8a)$$

where φ_{gel} is the volume fraction of the protein at the gel boundary. The protein mass concentration C_p is related to volume fraction φ by

$$C_p = \frac{\varphi M_w}{N_A v} \qquad (8b)$$

where M_w is the molecular weight of the protein, N_A is Avogadro's number, and v is the volume occupied by a single protein molecule.

Table 2. Values of Constants (M_w, N_A, v),[27,28] (d, Δ, σ)[23] and γ_e[26] for Protein Lysozyme Taken from the Literature

M_w	14 320 g/mol	Δ	0.3
N_A	6.023×10^{23}/mol	σ	3.4 nm
v	21.2 nm^3	γ_e	0.58
d	0.9		

Using approximations developed for particles experiencing short-range attractions[23−26] we can link solubility to the strength of attraction as

$$C_{sat.} = \frac{\rho_c}{\gamma_e}\exp\left(-\frac{\sqrt{3}\pi}{(1+d\Delta)^2}\frac{\epsilon}{kT}\right) \qquad (9)$$

where ρ_c is the crystal density, γ_e is the equilibrium activity coefficient, and d is a constant which is smaller than 1. Using eqs 8a and 8b and eq 9, we can express the protein mass concentration at the gel boundary ($C_{p,gel}$) as a function of salt concentration. Values for the constants used in the above equations, for the specific case of the protein lysozyme, were taken from literature[23,26−28] and are given in Table 2. The gel boundary thus obtained is shown in Figure 7 along with the

(18) Fine, B. M.; Lomakin, A.; Ogun, O. O.; Benedek, G. B. *J. Chem. Phys.* **1996**, *104*, 326−335.
(19) Rosenbaum, D.; Zamora, P. C.; Zukoski, C. F. *Phys. Rev. Lett.* **1996**, *76*, 150−153.
(20) Bergenholtz, J.; Fuchs, M. *J. Phys.: Condens. Matter* **1999**, *11*, 10171−10182.
(21) Bergenholtz, J.; Fuchs, M. *Phys. Rev. E* **1999**, *59*, 5706−5715.
(22) Bergenholtz, J.; Fuchs, M.; Voigtmann, T. *J. Phys.: Condens. Matter* **2000**, *12*, 6575−6583.
(23) Kulkarni, A. M.; Zukoski, C. F. *Langmuir* **2002**, *18*, 3090−3099.
(24) Sear, R. P. *J. Chem. Phys.* **1999**, *111*, 4800−4806.
(25) Christoffersen, J.; Rostrup, E.; Christoffersen, M. R. *J. Cryst. Growth* **1991**, *113*, 599−605.
(26) He, G. W.; Bhamidi, V.; Tan, R. B. H.; Kenis, P. J. A.; Zukoski, C. F. *Cryst. Growth Des.* **2006**, *6*, 1175−1180.
(27) Broide, M. L.; Tominc, T. M.; Saxowsky, M. D. *Phys. Rev. E* **1996**, *53*, 6325−6335.
(28) Poon, W. C. K.; Egelhaaf, S. U.; Beales, P. A.; Salonen, A.; Sawyer, L. *J. Phys.: Condens. Matter* **2000**, *12*, L569−L574.

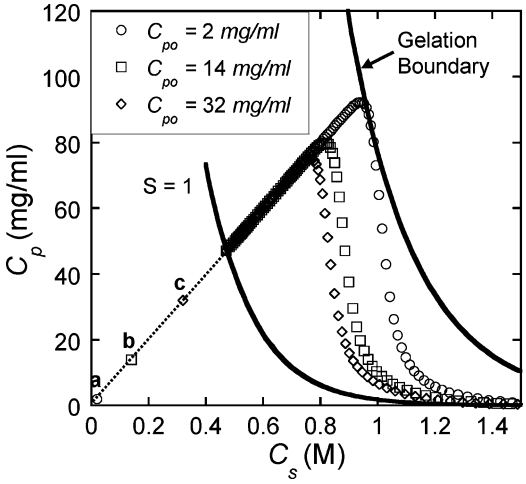

Figure 7. Lysozyme/NaCl phase diagram showing the gel boundary and the solubility boundary. Also shown is the protein/salt concentration profile of the evaporating drops for initial conditions corresponding to the data in Figure 4.

model-generated protein/salt concentration profile of the evaporating drops for initial conditions corresponding to the data in Figure 5. As per our hypothesis, we observe that for the case where $C_{p0} = 2$ mg/mL the protein concentration rises such that it crosses the gel boundary and forms a gel before nucleation and thus crystal formation can occur. The drops with the initial condition of $C_{p0} = 14$ mg/mL and $C_{p0} = 32$ mg/mL do not cross the gel boundary and result in crystal formation as shown in Figure 5b,c.

The kinetic parameters for lysozyme used in this work were derived using a different experimental setup where heterogeneous nucleation sites can be of different origin.[6] The agreement between our experimental crystal growth data and our model prediction using the parameters estimated by Saikumar et al. suggests that the nucleation processes are similar and thus may represent parameters associated with homogeneous nucleation or, if heterogeneous nucleation dominates in their experiments, it must dominate in ours too. Paxton et al. show that at high supersaturation homogeneous nucleation tends to dominate over heterogeneous nucleation.[29] In our experiment the maximum supersaturation typically exceeds 10, a range for which Paxton et al. estimate that homogeneous nucleation dominates.[29] Due to the high supersaturation achieved, we hypothesize that our experiments are dominated by homogeneous nucleation. The relative role of homogeneous and heterogeneous nucleation in producing crystals is not the focus of this work, however. On this point we conclude that the agreement between rate parameters derived form macroscopic experiments (Saikumar et al.) and microscopic studies (this work) suggests that similar nucleation mechanisms operate.

5. Conclusion

We used a kinetic model to simulate experiments performed in an evaporation-based crystallization platform using kinetic parameters for the crystallization of lysozyme as available in the literature. Excellent agreement is obtained for a wide range of drying rates and initial conditions between model predictions and experimental results. For the experiments described here the number of crystals is small, typically less than 10, since the volume of the individual droplets is on the order of only 5 μL. The model cannot reproduce the discrete nature of changes in the number of crystals observed at this level. Nevertheless, the ability of the model to predict crystal number in the range of ± 1 crystal suggests that this approach captures much of the underlying physicochemical processes giving rise to crystal nucleation and growth.

The remaining challenge is determination of the four kinetic parameters (k_n, k_g, a, and b) of crystal nucleation and growth using the crystal growth data obtained with the evaporation-based crystallization platform. An effort to estimate these kinetic parameters by finding the best fit of our model prediction to the experimental data demonstrated that these parameters are highly correlated, suggesting that the kinetic parameters of Saikumar et al. describe our system well but cannot be considered unique. A better understanding will be gained from experiments in which we can decouple the nucleation and growth events enabling us to estimate these parameters independently. At present we are developing an experimental protocol using the evaporation-based crystallization platform to provide independent measures of growth kinetic parameters. Subsequently, we will be able to extract accurate nucleation kinetic parameters in cases where both nucleation and growth occur at the same time.

LA063734J

(29) Paxton, T. E.; Sambanis, A.; Rousseau, R. W. *Langmuir* **2001**, *17*, 3076−3079.